An Analytical Upper-bound on the Benefits of Short-term Weather Forecasting for Ka-band (32 GHz)[1,2,3]

Shervin Shambayati
Jet Propulsion Laboratory
California Institute of Technology
4800 Oak Grove Drive
MS 238-420
Pasadena, CA 91109
(818)354-1280
shervin.shambayati@jpl.nasa.gov

Abstract— Due to spectrum limitations at lower frequencies, NASA's Deep Space Network is currently implementing Ka-band (32 GHz) tracking capabilities at all of its Deep Space Communication Complexes (DSCC's). Since weather effects and increases in the atmospheric noise temperature associated with them are the biggest uncontrollable factors in the performance of a Ka-band deep space telecommunications link, use of algorithms to forecast the atmospheric noise temperature for a pass is desirable. In this paper, an analytical method for comparing the performance of an ideal forecasting algorithm to the best statistical methods in terms of average data return is derived. This methodology is applied to two different cases. In the first case, the spacecraft cannot change its data rate during the pass. In the second case, the spacecraft can continuously vary its data rate. This methodology is applied to four different elevation profiles whose maximum elevation varies from less than 30 degrees to greater than 80 degrees for Goldstone, Madrid and Canberra DSCC's. This analysis shows that for the fixed data rate case, while the forecasting does not significantly increase the average data return on the link (between 0.2 dB and 0.4 dB, depending on the DSCC and the elevation profile) it does improve the reliability of the link significantly (in ideal case to 100%). For the continuously variable data rate case, forecasting improves both the average data return (by between 1 dB and 1.9 dB depending on the elevation profile and the DSCC) and the reliability of the link (in ideal case to 100%).

TABLE OF CONTENTS

I. INTRODUCTION
II. ANALYTICAL BACKGROUND
III. FIXED DATA RATE CASE
IV. CONTINUOUSLY VARIABLE DATA RATE CASE
V. NUMERICAL RESULTS
VI. CONCLUSIONS
ACKNOWLEDGMENT
REFERENCE

I. INTRODUCTION

Due to spectrum limitations at lower frequencies, NASA's Deep Space Network is currently implementing Ka-band (32 GHz) tracking capabilities at all of its Deep Space Communication Complexes (DSCC's). Since weather effects and increases in the atmospheric noise temperature associated with them are the biggest uncontrollable factors in the performance of a Ka-band deep space telecommunications link, use of algorithms to forecast the atmospheric noise temperature (ANT) for a pass is desirable. However, before any algorithms for ANT forecasting is evaluated, the overall value of such forecasts needs to be considered. In this document, a method for comparing the performance of an ideal prediction algorithm to the best statistical methods in terms of average data return is derived.

This paper is organized as follows: In Section II the analytical foundation of this paper is presented. In Section III the methodology for using predictions and optimizing the link statistically is presented for a fixed data rate case. In Section IV the methodology for variable data rate case is developed. In Section V the methodologies developed in Sections III and IV are applied to four sample passes for a 34-m Beam Waveguide (BWG) antenna for the three Deep Space Communications Complexes (DSCCs) and numerical results are obtained. In Section VI conclusions are reached.

[1] 0-7803-8155-6/04/$17.00 2004 IEEE
[2] This work is performed at JPL under a contract with NASA
[3] IEEEAC paper #0044, Version 1, Updated September 30, 2003

II. ANALYTICAL BACKGROUND

Before discussing the methodologies developed in this paper, it should be understood by the reader that DSN missions are typically tracked at elevations of greater than 10 degrees above the tracking station horizon. The period from the rise of the spacecraft above 10 degrees elevation to its setting below 10 degrees is considered the "view period" of the spacecraft. Some or all of the view period can be used to track the spacecraft. However, since the portion of the view period that is selected for tracking involves fiscal and scheduling issues and not just geometry, for the purposes of this paper, the entire view period is considered as tracking time. This will allows a fair and uniform comparison of different tracking methodologies.

Given a spacecraft configuration in terms of the transmitted power, the antenna gain and the pointing and the distance to the ground antenna, a link can support a data rate, R, provided that the ground antenna has a sufficiently high Gain to Noise Temperature Ratio (G/T). R is directly proportional to the minimum required G/T, γ, that is:

$$R = \alpha\gamma \tag{1}$$

For the purpose of this paper α is set to 1.

The actual G/T of the antenna depends on the elevation and the zenith atmospheric noise temperature (ANT). Given the fact that the system noise temperature is a random variable due to atmospheric effect then G/T of the antenna is also a random variable. Furthermore, since the ANT's probability distribution depends on the elevation at which it is observed and since the antenna gain varies with elevation, the probability distribution of G/T also varies with the elevation. To formalize this, let T_z be a random variable representing the zenith atmospheric noise temperature and let $\Gamma(\theta,T_z)$ be the function representing the antenna G/T at elevation θ given the zenith atmospheric noise temperature is T_z. Then we can define the survivor distribution function for $\Gamma(\theta,T_z)$ as:

$$\begin{aligned} F(\gamma,\theta) &= \Pr\{\Gamma(\theta,T_z) \geq \gamma\} \\ &= \Pr\{T_z < T_0\} \end{aligned} \tag{2}$$

where $\gamma = \Gamma(\theta,T_0)$. $F(\gamma,\theta)$ corresponds to the instantaneous availability of the link at elevation θ. We can also define an inverse function of $F(\gamma,\theta)$, $G(p,\theta)$ as:

$$G(p,\theta) = \{\gamma \mid F(\gamma,\theta) = p\} \tag{3}$$

Plotting $G(p,\theta)$ for a fixed value of p provides a tipping curve for the antenna. Note that when $\Pr\{T_z < T_0\} = p$, and p is expressed as a percentage, T_0 is referred to as p-percent weather. For example, 90-percent weather refers to a T_0 for which $\Pr\{T_z < T_0\} = 0.9$. Also note that for a fixed elevation, θ, $\Gamma(\theta,T_z)$ is a monotonously decreasing function of T_z since by definition $\Gamma(\theta,T_z)$ is the gain to system noise temperature ratio of the antenna at elevation θ and T_z contributes to the system noise.

Given the elevation profile for a pass, $\varphi(t)$, defined over time interval $(0,t_f)$ such that $\varphi(0) = \varphi(t_f) = 10^\circ$, then the average data return over the pass for a given data rate profile $\gamma(t)$ defined over $(0,t_f)$ is given by:

$$V_{\gamma,\varphi} = \int_0^{t_f} \gamma(t) F(\gamma(t),\varphi(t))\,dt \tag{4}$$

For a given $F(\gamma,\theta)$ Eq. (4) could be maximize with respect to $\gamma(t)$. Of course the data rate profile, $\gamma(t)$, is subject to limitations imposed by the spacecraft and ground system capabilities and operational policies. Let $\mathscr{G}$ be the set of all valid data rate profiles for the spacecraft over the time interval $(0,t_f)$. Then the optimum data rate profile, $\gamma_{opt}^{(\varphi)}(t)$, is defined as:

$$\begin{aligned} &\gamma_{opt}^{(\varphi)}(t) \ni \gamma_{opt}^{(\varphi)}(t) \in \mathscr{G}, \\ &V_{\gamma_{opt}^{(\varphi)},\varphi} \geq V_{\gamma,\varphi} \quad \forall \gamma(t) \in \mathscr{G} \end{aligned} \tag{5}$$

and the maximum data return volume is defined as:

$$V_{opt,\varphi} = \int_0^{t_f} \gamma_{opt}^{(\varphi)}(t) F(\gamma_{opt}^{(\varphi)},\varphi(t))\,dt \tag{6}$$

The set of valid data rate profiles, $\mathscr{G}$, could vary from mission to mission. However, for the purpose of this paper we concentrate on two sets of data rate profiles: fixed data rate profiles where the spacecraft can communicate with Earth only at a single data rate throughout the pass and the continuously variable data rate where the data rate changes continuously throughout the pass.

Of course, as mentioned above, this optimization depends on $F(\gamma,\theta)$. The way $F(\gamma,\theta)$ is selected depends on how accurately the weather could be predicted during the pass. In general, when no forecasting algorithm is used, $F(\gamma,\theta)$ is based on historical observations of the zenith atmospheric noise temperature. When a forecasting algorithm is used $F(\gamma,\theta)$ depends on the accuracy of the forecast. Let the random variable W taking values over an interval (w_0,w_1) with probability density function of $f_W(w)$ represent the quality of the weather as predicted

by the forecasting algorithm. Typically, W is the forecasted zenith atmospheric noise temperature. Furthermore, let $F(\gamma,\theta;w)$ be the probability survivor distribution function for G/T at elevation θ when the weather predictor forecasts a weather of quality w and let $\gamma_{opt}^{(\varphi)}(t;w)$ be the optimum data rate profile associated with this distribution for a pass whose elevation profile is given by $\varphi(t)$. Then the maximum amount of data that the link could return using this predictor for a pass with profile $\varphi(t)$ is given by:

$$V_{\varphi,\Omega} = \int_{w_0}^{w_1}\int_0^{t_f} \gamma_{opt}^{(\varphi)}(t;w)\, F\left(\gamma_{opt}^{(\varphi)}(t;w),\varphi(t);w\right) f_W(w)\,dt\,dw \tag{7}$$

When a perfect forecasting algorithm is used, W becomes the forecasted atmospheric noise temperature, T_0 and $F(\gamma,\theta;T_0)$ takes the form

$$F(\gamma,\theta;T_0) = \begin{cases} 1 & \gamma < \Gamma(\theta,T_0) \\ 0 & \text{otherwise} \end{cases} \tag{8}$$

This corresponds to $\Pr\{T_z = T_0\} = 1$.

Another near ideal weather forecaster is one that forecasts perfectly an interval of values for the zenith atmospheric noise temperature, *i.e.*, such predictor specifies an interval (T_m,T_n) such that $\Pr\{T_m < T_z < T_n\} = 1$ for the specified time of the forecast. This implies that such an algorithm forecasts an interval of G/T values at the time of the forecast such that $\Pr\{\Gamma(\theta(t),T_n) < \Gamma(\theta(t),T_z) < \Gamma(\theta(t),T_m)\} = 1$. Of specific interest in this paper is an n-percentile interval forecasting algorithm. This type of algorithm forecasts the zenith atmospheric noise temperature as belonging to one of $100/n$ intervals where n is an integral divisor of 100. Each interval, (T_{k-1},T_k), has the property that, in terms of the unconditional distribution of T_z, $\Pr\{T_z < T_k\} = \frac{n\cdot k}{100}$ for $0 \le k \le 100/n$. In the next two sections this algorithm will be used to approximate the performance of a perfect forecasting algorithm. It should be noted that both these algorithms guarantee 100% link availability since, according to the forecasts, the data rate could be set so that the link is always available.

III. The Fixed Data Rate Case

For the fixed data rate case the set of valid data rate profiles, $\mathcal{G}$, is limited to constant functions of time. When no forecasting is used, $F(\gamma,\theta)$ is based on the long term statistics of T_z. In this case Eq. (4) takes the form of

$$V_{\gamma,\varphi} = \int_0^{t_f} \gamma F(\gamma,\varphi(t))\,dt \tag{9}$$

The average availability over this pass is given by:

$$A_{\gamma,\varphi} = \frac{1}{t_f}\int_0^{t_f} F(\gamma,\varphi(t))\,dt \tag{10}$$

As the availability of the link could be quite low at lower elevations there may be a requirement that the spacecraft cannot be tracked unless the link is available more than p_0 fraction of the time. In this case Eq. (9) changes to

$$V_{\gamma,\varphi}^{(p_0)} = \int_0^{t_f} \gamma F(\gamma,\varphi(t))\, I_{p_0}\left[F(\gamma,\varphi(t))\right]dt \tag{11}$$

where $I_{p_0}(\cdot)$ is the indicator function of p_0 defined as

$$I_{p_0}(x) = \begin{cases} 0 & x < p_0 \\ 1 & x \ge p_0 \end{cases} \tag{12}$$

The average availability for this mode of operation is given by

$$A_{\gamma,\varphi}^{(p_0)} = \frac{\int_0^{t_f} F(\gamma,\varphi(t))\, I_{p_0}\left[F(\gamma,\varphi(t))\right]dt}{\int_0^{t_f} I_{p_0}\left[F(\gamma,\varphi(t))\right]dt} \tag{13}$$

Optimizing Eqs. (9) and (11) with respect to γ has been introduced before as Single Rate Optimization (SRO) [1][2] and Modified Single Rate Optimization (MSRO) [2], respectively.

When the link is limited to a single data rate during the pass, deriving equations for perfect forecasting is rather difficult. This is due to the fact that over the duration of the pass a perfect forecasting algorithm provides the actual G/T of the antenna during the pass as function of time. Since there is an infinite number of such functions that could be forecasted, there is no immediately obvious way to optimize for a single data rate. However, if it is assumed that the T_z does not change during the pass, a calculation of the average data return with perfect prediction could be made in the following manner. Suppose the forecasting algorithm forecasts a zenith atmospheric noise temperature of T_p for the pass. In addition, let probability that in general the zenith atmospheric noise temperature, T_z, is less than T_p be p (*i.e.*, if p is in percents then T_p corresponds to p-percentile weather.) Given T_p then the data return for the pass is given by:

$$V_{\gamma,\varphi}(p) = \int_0^{t_f} \gamma F(\gamma, \varphi(t); T_p)\, dt$$
$$= \int_0^{t_f} \gamma I_\gamma(G(p, \varphi(t)))\, dt \tag{14}$$

where $I_\gamma(\cdot)$ is the indicator function of γ defined similarly to $I_{p_0}(\cdot)$.

Maximizing Eq. (14) with respect to γ provides the optimum data rate to be used with the perfect forecasting algorithm. Let $\gamma_{opt,F}^{(\varphi)}(p)$ be the optimum data rate selected when the algorithm forecasts a zenith atmospheric noise temperature of T_p and let

$$V_{\gamma,\varphi}^{(opt)}(p) = \int_0^{t_f} \gamma_{opt,F}^{(\varphi)}(p)\, I_{\gamma_{opt,F}^{(\varphi)}(p)}(G(p, \varphi(t)))\, dt \tag{15}$$

Then the average data returned over this link with elevation profile $\varphi(t)$ is given by:

$$V_{\varphi,F} = \int_0^1 V_{\gamma,\varphi}^{(opt)}(p)\, dp \tag{16}$$

A lower bound approximation of Eq. (16) is given by:

$$V_{\varphi,F} \geq \sum_{k=1}^{100/n} V_{\gamma,\varphi}^{(opt)}\left(\frac{k \cdot n}{100}\right) \cdot \frac{n}{100} \tag{17}$$

Note that the right hand side of Eq. (17) is exactly the average data return provided by the *n*-percentile interval forecasting algorithm. Therefore, *n*-percentile interval forecasting algorithm could be used to approximate the performance of a perfect forecasting algorithm.

IV. Continuously Variable Data Rate Case

The equations for continuously variable data rate case are derived much more readily that those for the fixed data rate case. This is due to the fact that it is assumed that the data rate on the link could be changed instantaneously at any point during the pass.

When no forecasting is used, at any given elevation θ there is an optimum data rate $\gamma_{opt}(\theta)$ such that

$$\gamma_{opt}(\theta) F(\gamma_{opt}(\theta), \theta) \geq \gamma F(\gamma, \theta) \;\; \forall \gamma \tag{18}$$

Then for any elevation profile, $\varphi(t)$, the optimum data rate profile is given by:

$$\gamma_{opt}^{(\varphi)}(t) = \gamma_{opt}(\varphi(t)) \tag{19}$$

The average data return over the pass is given by

$$V_{opt,C}^{(\varphi)} = \int_0^{t_f} \gamma_{opt}(\varphi(t)) F(\gamma_{opt}(\varphi(t)), \varphi(t))\, dt \tag{20}$$

and the average availability over the pass is given by

$$A_{opt,C}^{(\varphi)} = \frac{1}{t_f} \int_0^{t_f} F(\gamma_{opt}(\varphi(t)), \varphi(t))\, dt \tag{21}$$

This optimization was introduced in [3] and is called Maximum Statistical Optimization (MSO). MSO provides an upper bound on the average data return over the link without the use of forecasting.

The data return equations for forecasting are also equally

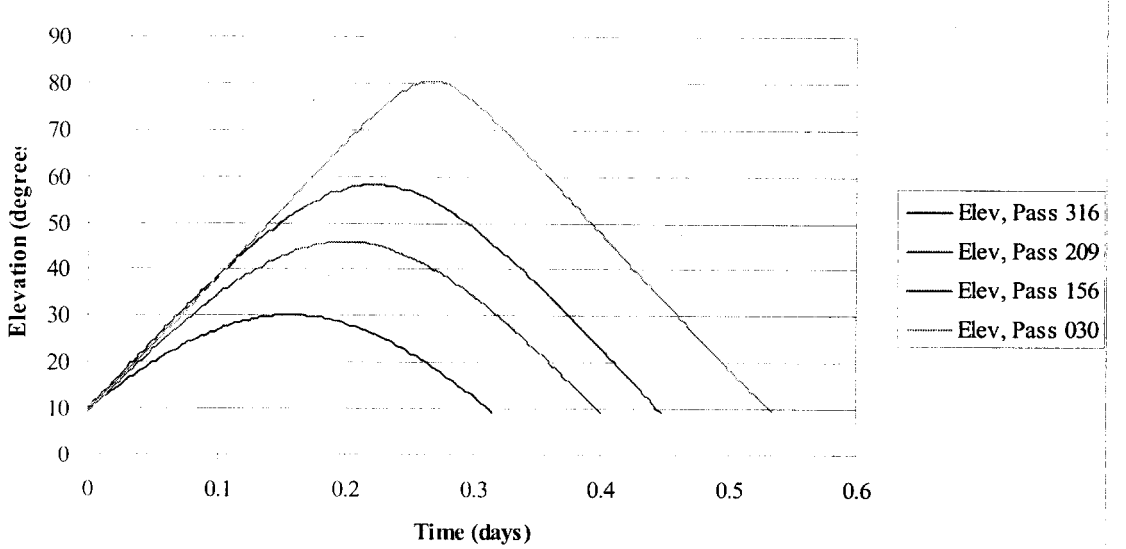

Figure 1. Elevation vs. Time, Passes 030, 156, 209 and 316

simple. Again suppose the forecasting algorithm forecasts a zenith noise temperature of T_p such that, in general, $\Pr\{T_z < T_p\} = p$. Then the maximum data rate that the link could support at the time of the forecast given that the elevation is θ will be $G(p,\theta)$. Therefore, the average data rate at elevation θ is

$$\bar{\gamma}(\theta) = \int_0^1 G(p,\theta)\,dp \tag{22}$$

Using Eq.(22), the average data return over the pass when perfect forecasting is used is given by

$$V_{\varphi,C} = \int_0^{t_f} \bar{\gamma}(\varphi(t))\,dt \tag{23}$$

Note that a lower bound for Eq. (22) is given by

$$\bar{\gamma}(\theta) \geq \sum_{k=1}^{100/n} G\left(\frac{k \cdot n}{100}, \theta\right)\frac{n}{100} \tag{24}$$

which is the average data rate at elevation θ for the n-percentile interval forecasting algorithm.

V. Numerical Results

In order to demonstrate the performance of methodologies presented in this paper, four representative passes over a 34-m Beam Waveguide (BWG) antenna are considered. The elevation profiles of these passes are shown in Fig.1. Using these elevations profiles along with the atmospheric noise temperature distributions for each of the DSN communication complexes and the models for the performance of the 34-m BWG antenna in [4], the performance of each methodology in terms of total data return and -when applicable- availability were calculated.

The results of applying the single data rate methodologies and forecasting are shown in Table I. As seen from this table the single rate optimized data volume is greater than the 90% MSRO data volume, by between 0.8 dB (pass 030, Goldstone) and 1.9 dB (pass 316, Canberra). This, however, comes at with cost of lower availability. As seen from Table III, the 90% MSRO provides an availability between 93.4% (pass 030, Madrid) and 97% (pass 156, Goldstone) while SRO provides an availability between 68.5% (pass 209, Canberra) and 76.2% (pass 316, Goldstone). As for the effects of prediction for the single rate case, as seen from Table I, the average data return is not greatly improved by forecasting over the SRO case and for some 10% Single Rate Prediction ($V_{\varphi,F}$, 10-percent) cases the average data return is actually less than that for the SRO. Therefore, for the single rate case it could be said that perfect weather prediction only improves the reliability of the link and not the average data return.

In order to apply the methodologies presented in this paper to continuous data rate case, first functions $G(p,\theta)$ and $\gamma_{opt}(\theta)$ needed to be calculated. Figs. 2, 3 and 4 show $G(p,\theta)$ vs. θ for different values of p for Goldstone, Madrid and Canberra, respectively. Fig. 5 shows $\gamma_{opt}(\theta)$ vs. θ for Goldstone, Madrid and

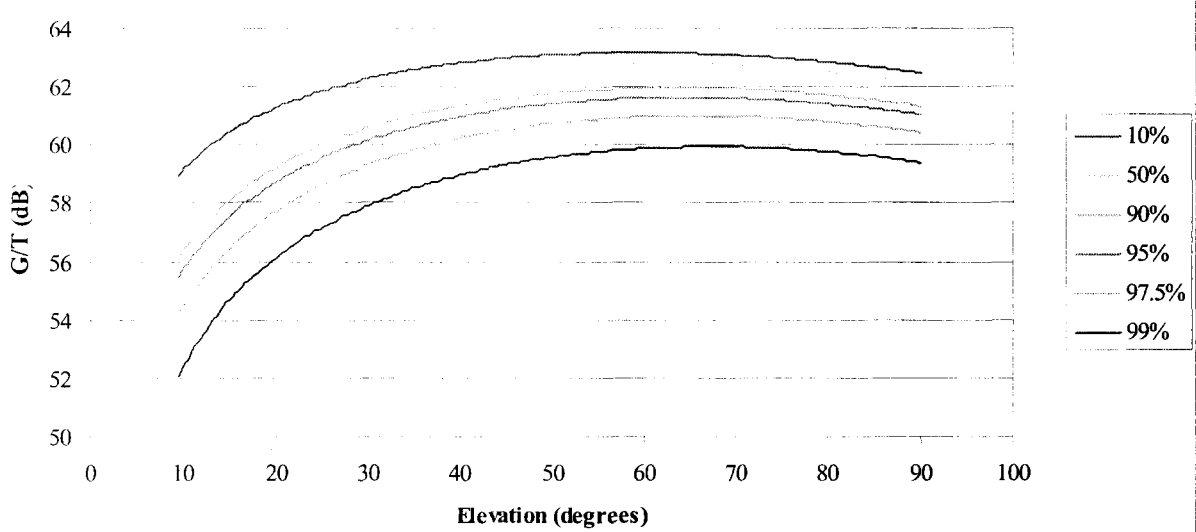

Figure 2. Ka-band Tipping Curves, 34m BWG, Goldstone

Canberra. The step jumps seen in this figure for all the curves are due to the fact that near the optimum value of γ for any elevation θ, the function $\gamma F(\gamma,\theta)$ is relatively flat (see Fig. 6). Therefore, the numerical methods used for calculation of $\gamma_{opt}(\theta)$ produce these steps. It should be noted, however, that the function $\gamma_{opt}(\theta)F(\gamma_{opt}(\theta),\theta)$ displays no discontinuities even when $\gamma_{opt}(\theta)$ does (see Fig. 7). Note that in Fig. 7 the highest $\gamma_{opt}(\theta)F(\gamma_{opt}(\theta),\theta)$ value for any elevation is obtained at Goldstone while the lowest is obtained at Canberra. This is due to the fact that of all three

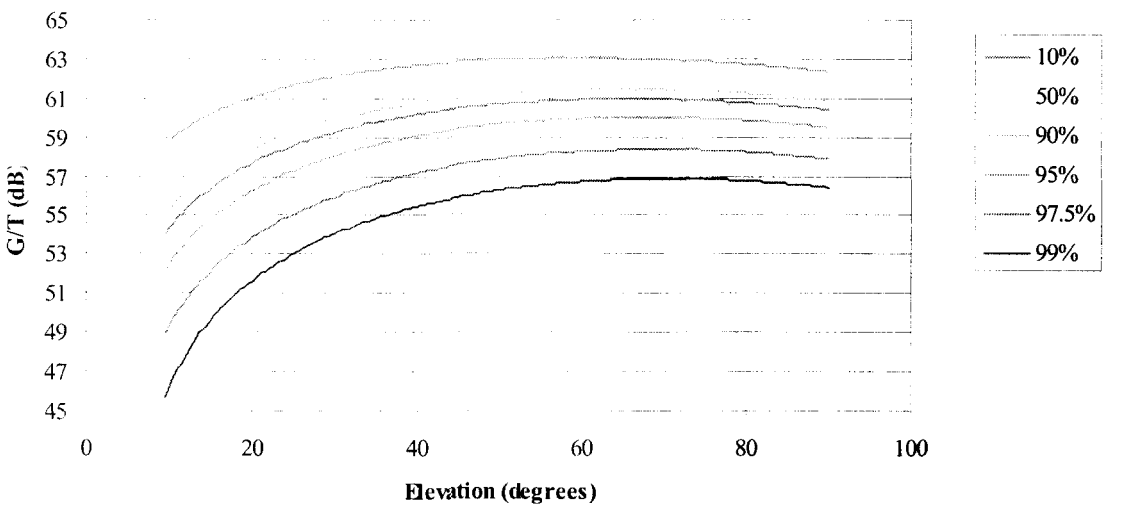

Figure 3. Ka-band Tipping Curves, 34m BWG, Madrid

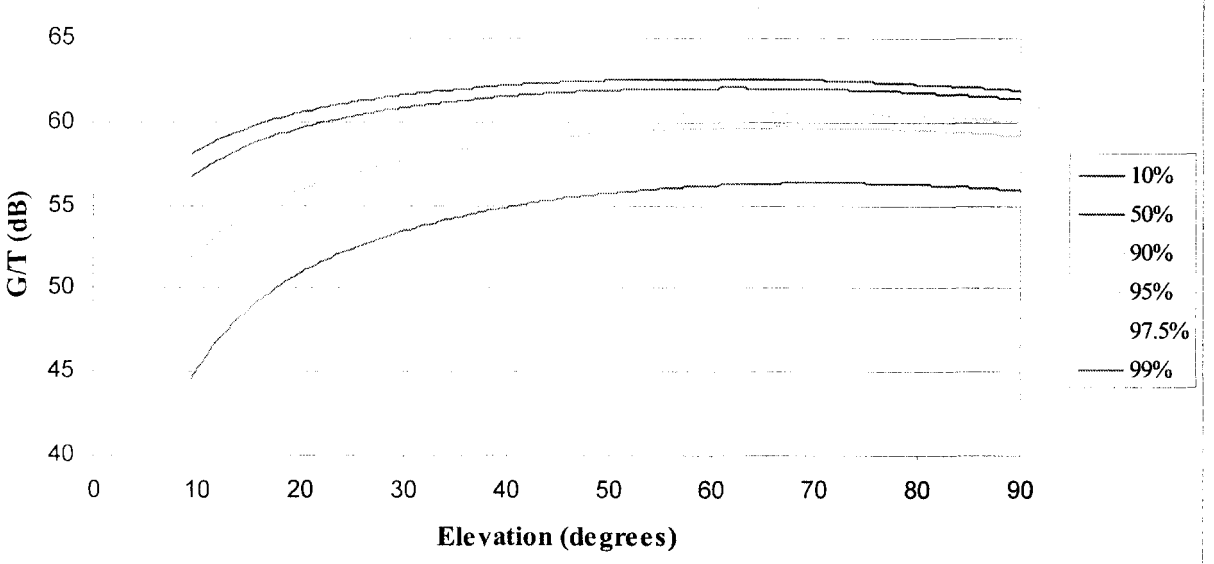

Figure 4. Ka-band Tipping Curves, 34-m BWG, Canberra

TABLE I. DATA RETURN OVER A 34-M BWG ANTENNA FOR DIFFERENT FIXED DATA RATE METHODOLOGIES

Pass	Site	90% MSRO	SRO	$V_{\varphi,F}$, 10-percentile Interval Forecasting	$V_{\varphi,F}$, 5-percentile Interval Forecasting	$V_{\varphi,F}$, 1-percentile Interval Forecasting
030	Goldstone	56.15	57.01	57.02	57.14	57.21
030	Madrid	55.44	56.55	56.59	56.73	56.82
030	Canberra	54.68	56.14	56.28	56.44	56.54
156	Goldstone	55.07	56.03	56.00	56.12	56.20
156	Madrid	54.34	55.55	55.53	55.68	55.79
156	Canberra	53.54	55.14	55.21	55.38	55.49
209	Goldstone	54.14	55.17	55.14	55.26	55.35
209	Madrid	53.38	54.66	54.66	54.81	54.90
209	Canberra	52.52	54.23	54.31	54.48	54.60
316	Goldstone	52.19	53.37	53.37	53.51	53.60
316	Madrid	51.32	52.81	52.82	52.98	53.10
316	Canberra	50.34	52.31	52.44	52.62	52.74

TABLE II. DATA RETURN OVER A 34-M BWG ANTENNA FOR DIFFERENT VARIABLE DATA RATE METHODOLOGIES

Pass	Site	MSO	$V_{\varphi,C}$, 10-percentile Interval Forecasting	$V_{\varphi,C}$, 5-percentile Interval Forecasting	$V_{\varphi,C}$, 1-percentile Interval Forecasting
030	Goldstone	57.67	58.72	58.83	58.89
030	Madrid	57.30	58.32	58.45	58.54
030	Canberra	56.69	58.05	58.20	58.30
156	Goldstone	56.76	57.86	57.97	58.04
156	Madrid	56.38	57.45	57.58	57.67
156	Canberra	55.75	57.16	57.31	57.41
209	Goldstone	55.89	57.06	57.18	57.25
209	Madrid	55.50	56.62	56.76	56.86
209	Canberra	54.85	56.31	56.47	56.58
316	Goldstone	53.92	55.24	55.37	55.45
316	Madrid	53.50	54.74	54.89	55.00
316	Canberra	52.79	54.39	54.56	54.68

TABLE III. AVERAGE AVAILABILITY OVER A34-M BWG ANTENNA FOR DIFFERENT STATISTICAL METHODOLOGIES

Pass	Site	90% MSRO	SRO	MSO
030	Goldstone	0.966	0.718	0.903
030	Madrid	0.934	0.691	0.860
030	Canberra	0.951	0.689	0.805
156	Goldstone	0.971	0.716	0.899
156	Madrid	0.943	0.687	0.858
156	Canberra	0.952	0.686	0.799
209	Goldstone	0.968	0.723	0.891
209	Madrid	0.941	0.690	0.853
209	Canberra	0.952	0.685	0.792
316	Goldstone	0.967	0.762	0.883
316	Madrid	0.939	0.718	0.845
316	Canberra	0.950	0.702	0.778

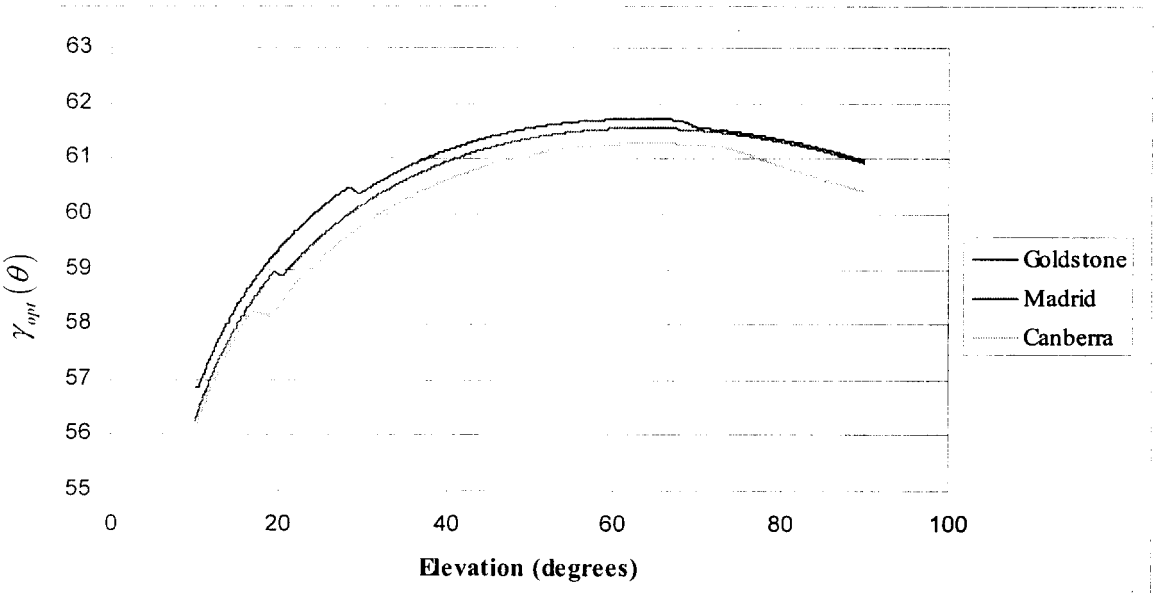

Figure 5. $\gamma_{opt}(\theta)$ vs. Elevation, 34-m BWG Antenna

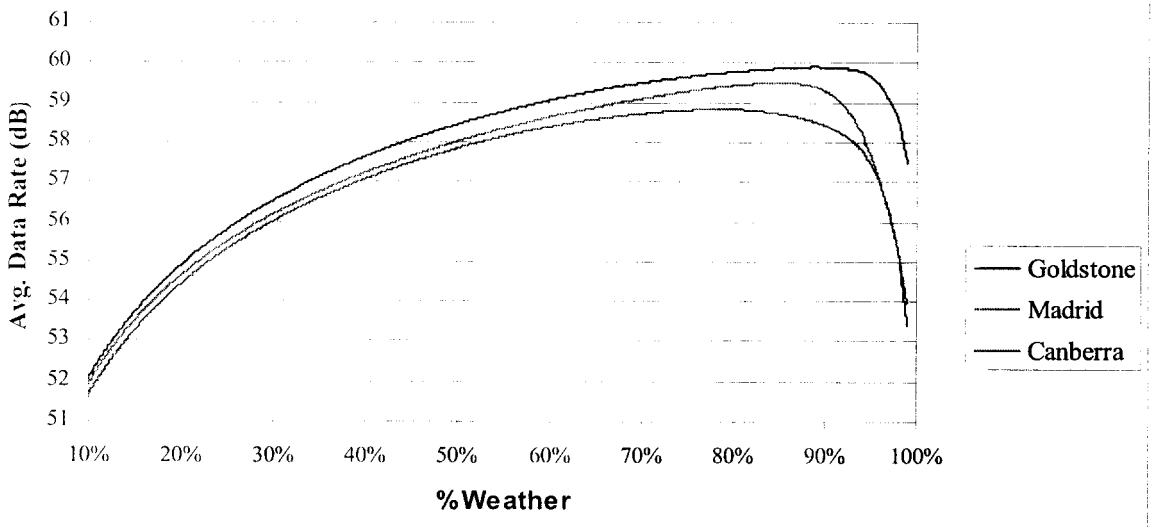

Figure 6. Ka-band $\gamma F(\gamma,\theta)$ (Average Data Rate) vs. $F(\gamma,\theta)$ (%Weather) for 34-m BWG Antenna

DSCC's Goldstone has the best weather and Canberra has the worst weather

The results of applying the variable data methodologies and predictions are shown in Table II. As seen from this tables, the MSO average data return is better than the SRO average data return by between 0.48 dB (Pass 316, Canberra) and 0.84 dB (Pass 209, Madrid) and better than 90% MSRO by between 1.52 dB (pass 030, Goldstone) and 2.45 dB (pass 316, Canberra). As seen in Table III, in terms of average availability MSO performs better than SRO and worse than 90% MSRO. The average availability for the MSO is about 90% for Goldstone, 85% for Madrid and 79% for Canberra. As seen from Table II, unlike the fixed data rate case, forecasting for the variable data rate improves the average data return over MSO by between 1 dB and 1.9 dB,

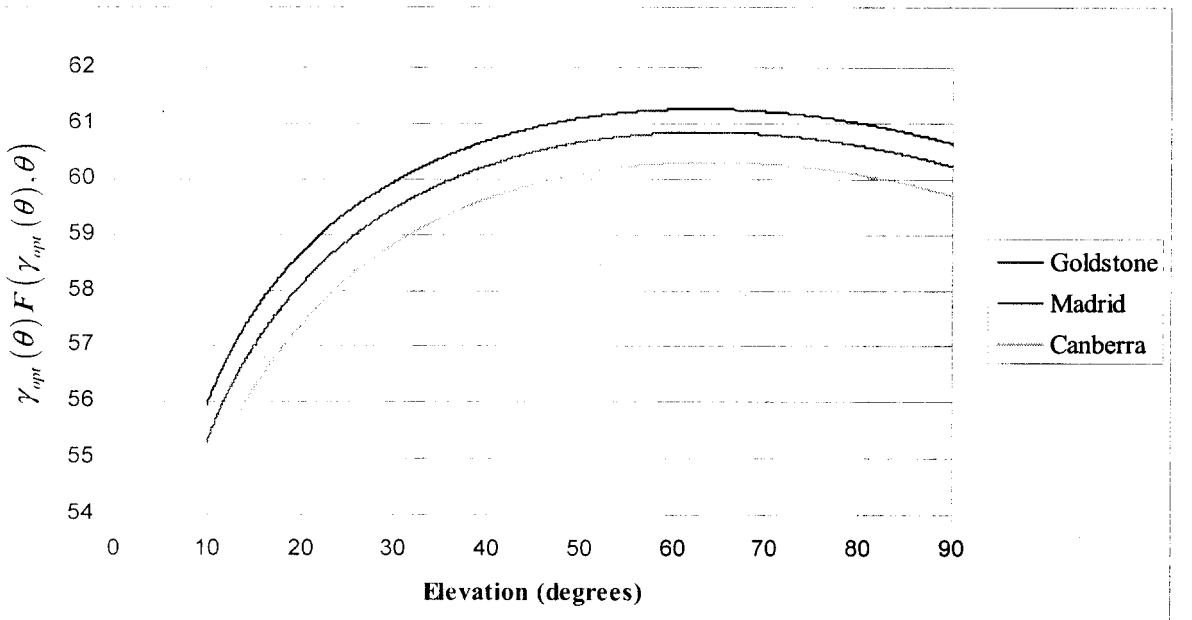

Figure 7. $\gamma_{opt}(\theta)F(\gamma_{opt}(\theta),\theta)$ vs. Elevation, 34-m BWG Antenna

depending on the pass, the location and the type of prediction. The reason that forecasts improve the average data return so significantly for the variable data rate case is that even with perfect forecasting the fixed data rate case is not able to use the whole duration of the pass. By contrast, the whole pass is available for use with the variable data rate case. Note that as the forecasting becomes more accurate (the size of the interval for n-percent interval prediction becomes smaller) the amount of data that is returned by the link increases.

VI. Conclusions

In this paper, methods for using perfect atmospheric noise temperature forecasting algorithms for deep space telecommunication links were introduced and their performance was compared with that of statistical link optimization methods at Ka-band for a 34-m Beam Waveguide antenna. It was shown that while a perfect predictor can improve the reliability of the link for a mission which cannot change its data rate during the pass, it cannot increase the average data return for that pass significantly over a statistically optimized single data rate link. However, if the spacecraft can vary its data rate continuously, the perfect forecasting algorithm not only increases the reliability of the link but also improves the average data return by 1 dB to 1.9 dB depending on the elevation profile of the pass and the Deep Space Communications Complex over which the spacecraft is being tracked. This implies that in order to fully take advantage of an atmospheric noise temperature forecasting algorithm the spacecraft needs to change its data rate during the pass.

Acknowledgment

The author would like to thank Dr. Samuel J. Dolinar of Jet Propulsion Laboratory for his helpful suggestions regarding the mathematical formulation of this problem.

Reference

[1] Shambayati, S., "Maximization of Data Return at X-band and Ka-band at DSN's 34-meter Beam-Waveguide Antennas," *IEEE 2002 Aerospace Conference,* Big Sky Montana, March 2002

[2] Shambayati, S., "Maximization of Data Return at X-band and Ka-band on the DSN's 34-meter Beam-Waveguide Antennas," *IPN Progress Report 42-148,* Jet Propulsion Laboratory, Pasadena, CA, February 15, 2002

[3] Shambayati, S., "On the Use of W-band for Deep Space Communications," *IPN Progress Report 42-154,* Jet Propulsion Laboratory, Pasadena, CA, August 15, 2003

[4] R. W. Sniffin, Ed., *DSMS Telecommunications Link Design Handbook (810-005, Rev. E),* Jet Propulsion Laboratory, Pasadena, CA, November 30, 2000

Shervin Shambayati obtained his Bachelors of Science degree in Applied Mathematics and Engineering in 1989 from California State University, Northridge. Subsequently, he obtained his MSEE, Engineer's Degree and Ph.D. from University of California, Los Angeles in 1991, 1993 and 2002, respectively. In 1993, Dr. Shambayati joined Deep Space Communications Systems Group at Jet Propulsion Laboratory where he took part in development and testing

of Deep Space Network's Galileo Telemetry receiver (DGT). In 1997, Dr. Shambayati joined the Information Processing Group at JPL where he has been working ever since. With that group Dr. Shambayati has been involved in various projects including Mars Global Surveyor's Ka-Band Link Experiment II, Deep Space 1 Ka-band testing and 70m antenna Ka-band Task. Dr. Shambayati's current research interests and activities include evaluating the effects of weather outage on the spacecraft resources, Ka-band weather forecasting, Ka-band link design for Mars Reconnaissance Orbiter and Mars Telecommunication Satellite and engineering support for implementation of Ka-band services in NASA's Deep Space Network.